Wojciech SAWCZUK, Bartosz PAGÓREK
POZNAN UNIVERSITY OF TECHNOLOGY, INSTITUTE OF COMBUSTION ENGINES AND TRANSPORT, DIVISION OF RAIL VEHICLES
3 Piotrowo Street, 60-965 Poznan

Compatibility of the λ- Kolmogorov test for the brake disc emissivity factor distribution in thermal imaging studies

Abstract

A thermal imaging camera is widely used in railway, it allows evaluating the wheel-rail contact while rolling the wheel set on the rails [3], cracks of the railway tracks [22] or identify overheated axle bearings of the wheel sets of the railway cars. In studies of braking systems both railway and vehicular ones on brake positions, the thermal imaging measurements are little used. Only in the qualitative assessment, an IR camera can identify the phenomenon of "hot spots" on the brake disc [1, 12, 15]. When testing the disc brake friction pairs, the most difficult is the brake disc and determination of its actual temperature which, due to the polished smooth surface by friction with the friction pad, is a low-carbon object. This type of objects force the person who makes the measurements to do a very precise configuration of the thermal imaging camera in order to determine the emissivity factor. An additional difficulty in the thermal imaging of braking systems is a dynamically changeable nature of the work associated with changes in the rotational speed of the brake disc and a non-linear increase in its temperature. The paper presents the results of the studies conducted parallel with the thermal imaging measurements by using thermocouples to determine variability of the experimental emissivity factor of the brake disc supported by the λ-Kolmogorov compatibility test.

Keywords: emissivity factor, brake disc, exponential distribution.

1. The methods of determining the emissivity factor

In order to accurately measure the temperature of an object by using a thermal imaging camera, it is necessary to compensate the different sources of radiation. It is done automatically by the camera after entering to its memory parameters like emissivity of the object, ambient temperature as well as reflected apparent temperature, camera distance, relative humidity and atmospheric temperature.

The most important parameter determining the reliability of temperature values, obtained in the research, is the actual thermal imaging emissivity of the surface. Other conditions may cause a measurement error in the range 1 or 2°C. The emissivity is defined as the ability to emit the radiation of an actual tested surface with respect to the ideal blackbody. It is equal to the ratio of the actual surface radiation intensity to the intensity of the blackbody radiation when assuming that both bodies have the same temperature [4]. This relationship is represented by the equation (1):

$$\varepsilon = \frac{W_{CR}}{W_{DC}} \tag{1}$$

where: W_{DC} – black body radiation, W_{CR} – Real body radiation.

The total capacity of the blackbody emission is the Stefan-Boltzmann law described by the equation (2):

$$W_{DC} = \sigma \cdot T^4 \tag{2}$$

where: σ – Stefan-Boltzmann constant ($\approx 5{,}67 \cdot 10^{-8}$ [W/m^2·K^4]), T^4 – temperature in Kelvin.

Polished (mirror) surfaces are characterized by emission below 0.1 while burnished surfaces or painted with black paint on the matte surface are best characterized by a factor of ε=0.98.

The simplest and quickest method for determining the factor is the use of emissivity tables for the tested material. A fragment of such an emissivity table is shown in Table 1.

Tab. 1. Emissivity table , T - total spectrum, SW - 2-5 μm LW- 8-14 . μm, LLW - 6,5-20 μm, 1 - material 2 - description 3 - temperature [C] 4 - spectrum, 5 - emissivity [3]

1	2	3	4	5
…	…	…	…	…
Iron and steel	electrolytic, carefully polished	175-225	T	0.05-0.06
Iron and steel	polished	100	T	0.07
Iron and steel	polished	400-1000	T	0.14-0.38
Iron and steel	shiny, pickled	150	T	0.16
Iron and steel	heavily rusted	17	SW	0.96
Iron and steel	strongly oxidized	500	T	0.98
…	…	…	…	…

It should be noted that the emissivity tables refer to particular values of temperature or temperature range of the material and the quality of its surface. In most cases, it is an oxidized surface (covered in black) or polished. In real studies, it is very difficult to choose an emissivity factor for materials not included in the table, as it is in the case of cast iron used in brake discs. In other emissivity tables [11, 13] for substances not defined as steel and cast steel or in the case of cast iron, the emissivity value is ε = 0.81 and temperature T = 50°C without specifying the surface type. Other sources [13, 14] indicate that for the polished iron ε=0.21 and for the raw casting ε=0.8 at the temperature of T = 0°C, even without specifying the nature of the surface (roughness of the surface). In [17, 18], the temperature of the cast iron of the brake disc was determined, but the measurement was made by measuring the temperature on the thickness of the brake disc not at the contact point with the brake disc. The obtained values were lower than those obtained from a measurement with thermocouples mounted 1 mm into the material of the brake disc as prescribed by the standard [16] in the research of railway brake discs.

Another frequently used method to determine the emissivity of the tested element is the method using black electrical tape with known emissivity. In this method, an IR camera is configured in terms of the measured apparent temperature, atmosphere, humidity and the distance from the object. The insulation tape is glued on the tested object. Then, in the thermal imaging camera the emissivity of 0.97 is intentionally introduced and the temperature of the tape, by using the function as an isotherm, is measured, point (straight) or rectangle. It is recommended, according to [4], to heat the object to a temperature higher by 20°C relatively to the ambient temperature. After writing the temperature on the black sample, the IR camera is moved to another area of the object (of varying roughness and color) and the emissivity in the camera is adjusted as long as the temperature will be the same as in the place with the black tape on the object.

In the case of brake discs, the said method can only determine the emissivity at a low disc temperature of about 50°C, having regard to a surplus of the object temperature relatively to the ambient temperature. However, due to the fact that the range of operation of the brake disc at higher temperatures averages 200-400°C, for the iron, depending on the simulated speed of braking and because of changes in roughness of the disc surface - the value of the emissivity will be different than that at a lower temperature. In [10], there are presented the results of laboratory tests which

determined the dependence of ε of the brake on the braking process parameters. The study explained the change of emissivity by means of precipitation of the friction material on the brake disc.

The rest of the paper shows the method of determining the actual value of the ε coefficient, in a dozens of braking series with additional thermocouples mounted on the brake disc.

2. The research methodology

Research of the disc brake evaluation was conducted on a brake position at the Institute of Rail Vehicles TABOR in Poznan. The position allows conducting a test of the block brake and the disc brake. The proving reflects the actual conditions that occur during car or traction vehicle braking. The study covered a disc brake, consisting of brake discs with the outer diameter of 590 and 640 mm and ventilation blades and a set of the friction pads of type 175 and 200 FR20.H.2. with a thickness of 35 mm.

The research of the brake disc temperature was conducted by using six thermocouples installed on the disc, three on each side of the disc. During the research an IR camera was also used.

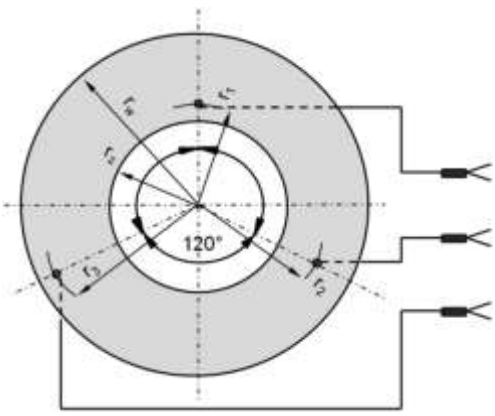

Fig. 1. View of thermocouples distribution on the brake disc in accordance with the [16]

The holes for thermocouples (∅2,5mm) were drilled at 120^0 on three rays of the disc, $r_1 = r_w + ¼ (r_z - r_w)$, $r_2 = r_w + ½ (r_z - r_w)$, and $r_3 = r_w + ¾ (r_z - r_w)$ (r_z- outer radius of the disc, r_w - radius of the inner disc), as shown in Figure 1.

Thermocouples against the friction surface of the disc were embedded 1 mm in the disc so that the ends of thermocouples, according to [16] were not destroyed by the friction pad. In the holes which were close to the outer diameter of the disc, the thermocouples with the longest operating part were installed (TP-213K-a-300-200 thermocouples). On the other rays, TP-213K-A-200-200 thermocouples were installed. On the other side of the disc, there were holes shifted by 60^0 in relation to the first side in order to avoid overlapping of thermocouples. The method of temperature measurement by using thermocouples and an infrared camera is shown in Figure 2. In the position test, which is not a requirement of UIC 541-3 card, the FLIR thermal imaging camera E60 was used. It was used for the qualitative assessment of the braking process.

The position tests for the railway brakes were carried out in accordance with one of the programs contained in the UIC 541-3 card. Parameters for the 2B program, of the tests were as follows:
– pressure of the pad to the disc p=25 kN,
– beginning of the braking speed: v=120 km/h,
– braking mass per one disc: M=5.7 t.
– temperature of the disc at the beginning of braking T=100°C.

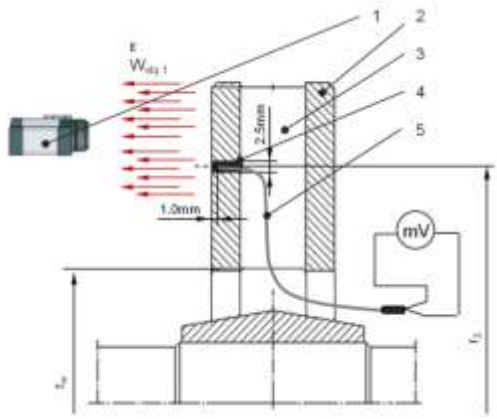

Fig. 2. Research methodology of the brake disc temperature: 1-IR camera, 2-friction ring, 3-ventilating blade 4- elastic bush, 5- TP-213K-a-200-200 thermocouple, r_w-inner radius r_3- thermocouple assembly ray , ε-emissivity, $W_{obj.}$1,2-radiation of the object 1, 2

A view of the brake disc with mounted thermocouples and thermal imaging camera used for tests of the average temperature distribution of the disc brake is shown in Figure 3.

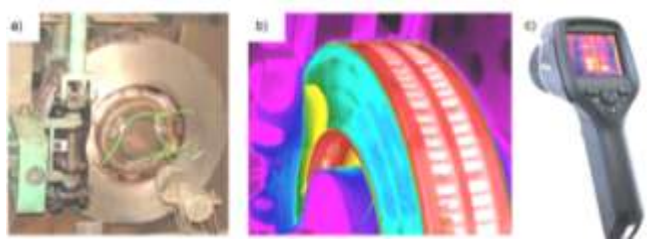

Fig. 3. Temperature measurement of the disc brake systems: a) thermocouples installed on the disc friction ring, b) thermal image of the disc brake system, c) thermal imaging camera FLIR E60

Tab. 2. Values of the thermal imager configured for stand tests disc brake

Emissivity	0.97
Reflected apparent temperature	18˚C
Distance	2 m
Relative humidity	50%
Air temperature	18˚C
Temperature of the external optical system that it	20˚C
Transmission of the optical external system	1.0

The study was divided into two phases. In the first stage, due to the lack of information about the real value of the emissivity factor, the coefficient ε=0.97 was entered to the camera because of the fact that the brake disc was coated with a black heat-resistant paint on its thickness, including ventilation ducts. Later the temperature was read from these surfaces. Other parameters like temperature of the atmosphere and reflection, humidity and the distance from the object (disc) were entered to the camera and the values are shown in Table 2. At this stage, thermal images of the disc brake were recorded on the brake position, and the temperature of the friction surface of the disc with 6 thermocouples was recorded simultaneously. Thermal images were taken in the stop time, measuring Tk - the temperature of the end of braking by the use of thermocouples and thermal imaging camera. Thermocouples were chosen based on [16]. The accuracy of temperature measurement using thermocouples on a validated brake according to [7] did not exceed 1%.

In place of study of the brake disc, there was no other source of heat, the engine driving position was separated by a cover and rotating masses and located at a distance of 5.5 m [7]. In addition, the test disc brake was protected from the environment three walls (front, rear and top), while on the left side there was additional protection from the rotating masses (Fig. 4b). In addition, during the study using the infrared camera illumination position was switched off.

The temperature of the components located in the vicinity of the brake disc (e.g. elements of lever mechanism) did not exceed 30° C because of the forced cooling air to simulate movement of the train before braking in accordance with [9]. It should be stressed that more inhibition was followed by the descending disc at 50°C.

In the second stage, thermal images were modified in FLIR Tools software. Then, on the working surface of the disc (contact surface with the friction pad), an ellipse was marked (see Figure 4), calculating the average value of the temperature from the polished surface. Next, based on the results of the temperatures recorded by the thermocouples attached to the friction surface, the emissivity value was changed in FLIR Tools software. It was made to get the same temperature of the disc friction surface as in the case of thermocouples. This is the method described in the [21].

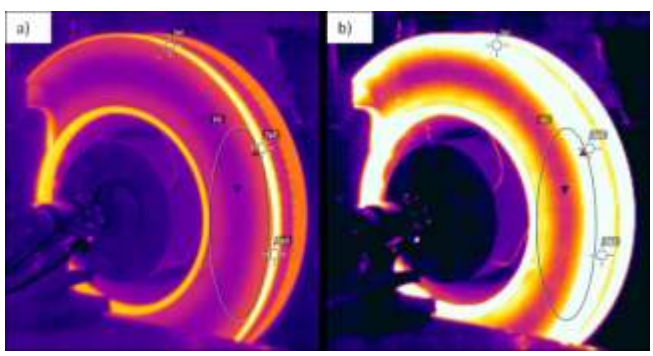

Fig. 4. Thermographic image of the FLIR E60 camera generated in the FLIR Tools: a) for 0,97 value of the emissivity, b) for emissivity amended

Figure 4 shows an example of the thermal image of the brake disc in order to determine the real value of the emissivity. Analyzing Figure 4a) one can recognize that the temperature at the friction surface of the rail brake disk is lower than in the central portion (the fan blades). It is associated with several medium. Firstly, the braking friction surface cools faster because of the forced air in the front brake disc. In addition, the phenomenon of thermal conduction is a phenomenon, thus slow register 50°C before braking the thermocouple does not mean that the entire disc is cooled to that temperature. The thickness of the rail brake disc in accordance with [16] is 110 mm, which can cause the higher temperature of the central portion. The central part of the shield has a rough surface to the casting and in addition to the introduction of fixed (constant) values of emissivity (ε = 0.97), it was painted with black heat-resistant. Only in a subsequent step of image analysis in the FLIR Tools, the emissivity was changed to the temperature of the thermocouple and was the same as the area marked on the disc in the FLIR Tools.

3. Research results

During the tests, 70 brakes were investigated. The tests were conducted in the same initial conditions, i.e. at the same braking speed, pads pressure to the disc, braking mass and the temperature of the beginning of the braking. By changing the emissivity factor in FLIR Tools, the same values of disc temperature, measured by the use of the thermocouples and IR camera were obtained. The values of the ε factor in the subsequent brakings are shown in Figure 5.

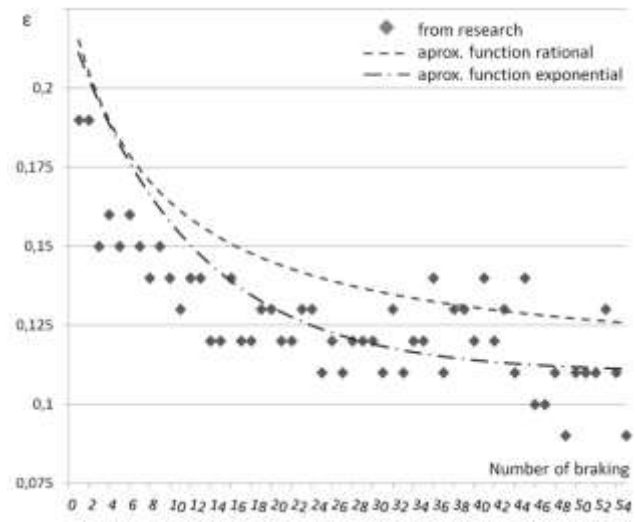

Fig. 5. Change of the coefficient of variation in subsequent brakings in unchanged initial conditions. The dashed line represents a rational function, dotted line - the exponential function

This was followed by approximation for different functions describing a change of the variation in the subsequent brakings by the highest value of the coefficient of determination according to the equation (3):

$$R^2 = \frac{\sum_{p=1}^{n}\left(\hat{y} - \bar{y}\right)^2}{\sum_{p=1}^{n}\left(y_t - \bar{y}\right)^2} \tag{3}$$

where: $\hat{y}$ – predicted value based on the model, $\bar{y}$ – average value, y_t – real value.

The highest values of the coefficient of determination R^2 was obtained for two functions describing the change of the emissivity factor in the next brakings. It is a rational function described by equation (4), and the exponential function described by equation (5).

$$y_{\varepsilon 1} = \frac{1}{P+7} + 0{,}11 \quad R^2 = 0{,}700 \tag{4}$$

$$y_{\varepsilon 2} = 0{,}11\left(1 + e^{-\frac{p}{12}}\right) \quad R^2 = 0{,}995 \tag{5}$$

where: p– Number of the next braking p = 1, 2, 3, ...

Both functions described in equations (4) and (5) approach asymptotically the value of 0.11 which corresponds to the normalized emissivity in the next brakings. However for further analysis, an approximating $y_{\varepsilon 2}$ exponential function was used because of the higher R^2 rate. On the basis of these studies it was found that after 40 brakings the coefficient value stabilized at the value of 0.113, obtained from the arithmetic mean of 30 brakes, i.e., calculated from the 41th brake to the 70th brake.

Figure 6 presents the average values of 10 brakings carried out one after another in a series of 70 brakings. Additionally, the error bars with a standard error are indicated on the graph.

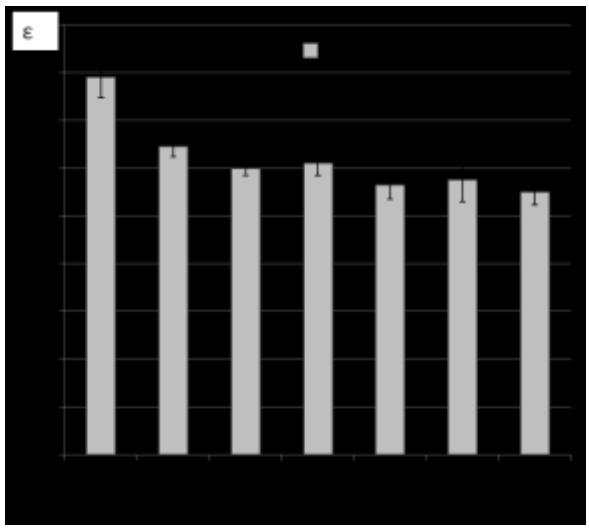

Fig. 6. Comparison of the average emissivity factor values of the brake disc from the tests on the braking position, from the next 10 brakings written as 1-10. It means that it is the average value from brakings from 1 to 10

4. Compatibility of the λ-Kolmogorov test for the distribution of the brake disc emissivity factor

The purpose of conducting the λ-Kolmogorov compatibility test is a hypothesis that the tested trait, i.e. a change in the emissivity of the brake disc, specified a theoretical distribution in the general population. The general population consisted of 70 brakings (n=70) on the braking position. For this population, 13 intervals with a width of 0.011 were established, as the maximum value of emissivity for this population was 0.18 and the lowest value – 0.008 which gave a gap of 0.1. With the 13 class intervals, it was possible to construct the histogram at which the value changed every 0.011.

Using equations (6-7), the average value and standard deviation for the emissivity were calculated. They respectively were μ=0.1237 and S=0.01889, for the population of 70 measurements. The average value

$$\bar{x} = \frac{1}{n}\sum_{i=1}^{n} x_i \tag{6}$$

where: x_i – i- this value is variable, x = 1, 2, ..., n, n – number of measurements.

The standard deviation:

$$S = \sqrt{\frac{1}{n}\sum_{i=1}^{n}(x_i - \bar{x})^2} \tag{7}$$

where: $\bar{x}$ – average value, x_i – i - this value is variable, x = 1, 2, ..., n.

The size distribution of the coefficient ε during the subsequent brakings, as shown in Figure 6, is approximated by a normal N distribution with an average μ and S equivalent to δ^2 standard deviation variance.

The coefficient of determination R^2 calculated from the equation (3) of the adjustment of the ε histogram distribution, measured relatively to the normal distribution N, was 0.947.

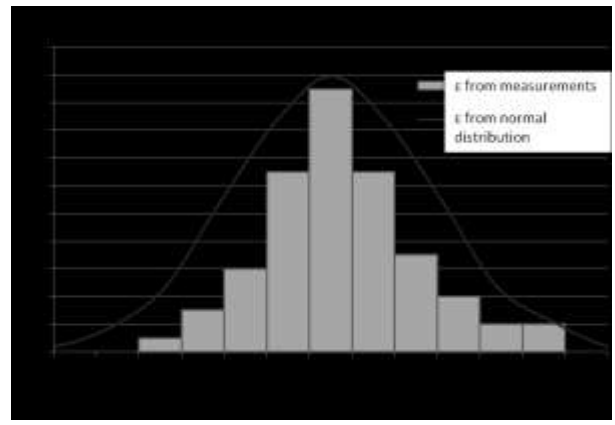

Fig. 7. Comparison of the emissivity factor distribution number relatively to the 13 interval classes

On the basis of Figure 7, we hypothesized that the tested characteristic, i.e. the distribution of the emissivity of the brake disc, has 70 measurements and the normal distribution N (0.1237 0.01889) in a given population, is described by equation (8) [5, 8]

$$f(x) = \frac{1}{\sqrt{2\pi}S} e^{\frac{-(x-\mu)^2}{2S^2}} \tag{8}$$

The cumulative distribution of the exponential distribution is given by relationship (9) [5, 8]:

$$F(x) = \int_{-\infty}^{x} \frac{1}{\sqrt{2\pi}S} e^{\frac{-(x-\mu)^2}{2S^2}} dx \tag{9}$$

The λ-Kolmogorov Compatibility Test was carried out under the following conditions [2, 6]:

1) the distribution of the general population with a continuous random variable F distribution function was optional.
2) a sample size $n \geq 6$.

The following hypothesis were made:

1) $H_o : F = F_o$,
2) $H_1 : F \neq F_o$.

To verify the hypotheses, the following statistics described by equations (10) and (11) [2, 6] were used:

$$U = D_n \cdot \sqrt{n} \tag{10}$$

$$D_n = \max\left|F_n(x_i) - F_o(x_i)\right| \tag{11}$$

where: $F_n(x_i)$ - empirical cumulative distribution function of the normal distribution, $F_o(x_i)$ - theoretical distribution function of the normal distribution.

The critical area for the λ-Kolmogorov test is given by the relationship (12) [2, 6]:

$$R_\alpha = (K_{1-\alpha}, \infty) \tag{12}$$

where: $K_{1-\alpha}$ - quantile of the Kolmogorov limiting distribution.

The method of determining the statistic U is presented in Table 3. Figure 8 shows the distribution course of the theoretical and empirical normal distribution N.

Tab. 3. Verification of the hypothesis Ho with the λ-Kolmogorov compliance test, the change of the emissivity factor of the brake disc has 70 braking in a given population and the normal distribution N (0.1237 0.01889)

Lp.	x_d - x_g	n_i	$F_n(x_g)$	n_{isk}	$F(x_g)$	$F(x_g)$-$F_n(x_g)$	
1	(0.047-0.058>	0	0	0	0.0010	0.0010	
2	(0.058-0.069>	0	0	0	0.0054	0.0054	
3	(0.069-0.080>	1	0.0143	1	0.0252	0.0109	
4	(0.080-0.091>	3	0.0571	4	0.0778	0.0207	
5	(0.091-0.102>	6	0.1429	10	0.1997	0.0568	
6	(0.113-0.124>	13	0.3286	23	0.3861	**0.0575**	maxD_n
7	(0.124-0.135>	19	0.6	42	0.6092	0.0092	
8	(0.135-0.146>	13	0.7857	55	0.7956	0.0098	
9	(0.146-0.157>	7	0.8857	62	0.9174	0.0317	
10	(0.157-0.168>	4	0.9429	66	0.9700	0.0272	
11	(0.168-0.179>	2	0.9714	68	0.9946	0.0232	
12	(0.179-0.190>	2	1	70	0.9990	0.0010	
13	(0.190-0.201>	0	1	70	1	0.0000	

n_i- number of observations,
n_{isk}- cumulative numbers

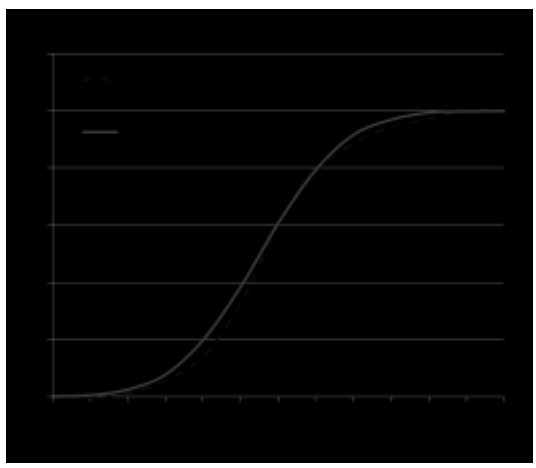

Fig. 8. Fig. 8 Empirical and normal distribution function for changing the emissivity factor of the brake disc.

With the biggest difference in the distribution of empirical and theoretical function which is 0.0575, the tested function was calculated according to equation (10), which was:

$$U = 0{,}0575 \cdot \sqrt{70} = 0{,}48$$

The critical area was evaluated on the level of significance α = 0.01. From tables included in [6] the Kolmogorov limiting quanta distribution:

$$K_{1-\alpha} = 0.192$$

because

$$U \in (K_{1-\alpha}, \infty)$$

Fig. 9. Graphic representation of the test function and the critical area for three levels of significance

The H_0 Hypothesis (read: the random variable which is an emissivity factor of the brake disc), has in a given population 70 measurements and the normal distribution N (0.1237 0.01889) has to be rejected.

5. Conclusions

In this paper, there is assessed the variability of the emissivity factor of the brake disc as a low-carbon object. The study and review of the literature indicate a variability of ε coefficient in subsequent measurements (i.e. in the next brakings carried out in constant, initial conditions). The obtained results show that the emissivity factor can be approximated by the exponential function represented by equation (5) with a high coefficient of determination R^2 = 0.995. The studies carried out on the braking position showed that the ε coefficient changed from 0.18 and stabilized at a value of 0.11, which is included in emissivity tables presented in some guidebooks or in polished steel articles. However, it should be noted that the value of 0.11 is obtained after a few brakings (in these tests after 30 brakings) at a temperature of about 170-180°C of the brake disc, measured with thermocouples during the stop time. The main cause of variability of the emissivity factor should be explained, which is already reported in the literature, by transferring the friction material to the brake disc and change of the brake disc roughness in the first brakings. A cast brake disc is turned to size and in subsequent brakings the friction surface is similar to the polished one. The next stage is to find a dependence of the emissivity factor on the surface roughness measured by Ra parameter. Then more accurate determination of the thermo-mechanical model will be possible, not only dependent on the number of brakings.

The practical aspect of the analyzes of infrared images is to develop a non-linear model of the emissivity (thereby giving its dispersion). In addition, equation (5) allows you to specify the number of brakings after the ε ratio stabilizes at a constant level. Another practical aspect of research conducted on the brake disc using a thermal imaging camera is the ability to identify surface defects on the disc such as surface cracks. A simpler method of indirect measurement of the temperature of the target is the measurement on high-emission parts on e.g. on its thickness. In [17, 18], it is shown, however, that the main limitation of this method is the need to introduce correction coefficients that allow converting the temperature with thick blades or a forced ventilation temperature friction ring.

In the second part of the paper, an attempt to present the variability of emissivity with the N normal N distribution with an average μ and standard S deviation was made. However, the test of λ-Kolmogorov, conducted on a sample of 70 brakings did not show clearly that this is a normal distribution. We could only assume an empirical distribution despite the high coefficient of determination R^2=0.94 and adjustment of the empirical distribution to the normal distribution with the arithmetic mean of 70 measurements μ=0.1237 and S=standard deviation of S=0.01889

The project is funded by the National Centre for Research and Development, program LIDER V, contract No. LIDER/022/359/L-5/13/NCBR/2014.

6. References

[1] Belhocine A., Bouchetara M.: Thermomechanical modelling of dry contacts in automotive disc brake. International Journal of Thermal Sciences 60 (2012), pp. 161-170.
[2] Bobowski Z.: Wybrane metody statystyki opisowej i wnioskowania statystycznego. Wydawnictwo Wałbrzyskiej Wyższej Szkoły Zarządzania i Przedsiębiorczości. Wałbrzych 2008.
[3] Coleman I., Kassa E., Smith R.: A Multi-Point Contact Detection Algorithm Combined with Approximate Contact Stress Theories, Proceeding of the First International Conference on Railway

Technology: Research, Development and Maintenance, J. Pombo (Editor), Civil-Comp Press, Stirlingshire, Scotland, Paper 139.
[4] FLIR Exx Instrukcja obsługi. Publ. No. T559662 Rev. a572 – POLISH (PL) – November 7, 2011.
[5] Gajek L., Kałuszka M.: Wnioskowanie statystyczne – modele i metody. Wydawnictwo Naukowo-Techniczne Warszawa 2000.
[6] Kadziński A.: Niezawodność pojazdów szynowych. Wydawnictwo Politechniki Poznańskiej, Poznań 1992.
[7] Kaluba M.: Nowoczesne bezwładnościowe stanowisko do badań hamulców pojazdów szynowych. Pojazdów Szynowych, Poznań 2004, nr 1, s. 22-28.
[8] Kałuszka K.: Elementy statystyki w zadaniach. Wydawnictwo Naukowe PWN, Warszawa 2007.
[9] Karta UIC 541-3: Hamulec: hamulec tarczowy i okładziny hamulcowe, warunki ogólne dla prób na stanowisku badawczym, Wydanie 6-te listopad 2006, s. 17-18.
[10] Kurczek T., Kowal L., Turewicz K., Ścieszka S.F., Żołnierz M.: Wybrane aspekty termowizyjnych pomiarów temperatury tarczy podczas eksperymentalnych badań hamulców tarczowych, Pomiary Automatyka Kontrola, 9/2013, s. 969-972.
[11] Kwiatkowski A., Smulko J.: Metody usuwania zakłóceń podczas pomiarów polowych widm Ramana. Pomiary Automatyka Kontrola 4/2013, pp. 281-284.
[12] Li Z., Han J., Yang Z., Li W., Analyzing the mechanisms of thermal fatigue and phase change of steel used in brake discs. Engineering Failure Analysis 57 (2015), pp. 202-218.
[13] Minkina W., Dudzik S.: Infrared Thermography: Errors and Uncertainties. Wydawnictwo Chichester: John Wiley and Sons, Inc., 2009. pp. 192.
[14] Morawski R., Miękina A.: Monte-Carlo evaluation of measurement uncertainty using a new generator of pseudorandom numbers. Pomiary Automatyka Kontrola 5/2013, pp. 390-294.
[15] Panier S., Dufrénoy, Weichert D.: An experimental investigation of hot spots in railway disc brakes, WEAR 256 (2014), pp 764-773.
[16] Polska Norma PN-EN 14535-1, Kolejnictwo – tarcze hamulcowe kolejowych pojazdów szynowych – Część 1: Tarcze hamulcowe wtłaczane lub mocowane skurczowo na osiach zestawów tocznych lub napędnych, wymiary i wymagania dotyczące jakości, Warszawa 2006.
[17] Sawczuk W.: The evaluation of a rail disc brake braking process by using a thermal camera, Measurement Automation Monitoring, No 6/2015, pp. 265-270.
[18] Sawczuk W., Tomaszewski F.: Ocena rozkładu średniej temperatury pary ciernej tarcza hamulcowa-okładzina z obsadą hamulcową w czasie hamowania ze stałą mocą. Pomiary Automatyka Kontrola, 9/2013, s. 938-941.
[19] Website: http://www.mera-sp.com.pl/rozwiazania/wiecej/pirometry-poradnik-uzytkowania
[20] Website: http://termo-sfera.pl/termowizja/przykladowe-wartosci-wspoczynnikow-emisyjnosci.html
[21] Więcek B, De Mey G.: Termowizja w podczerwieni podstawy i zastosowania. Wydawnictwo PAK, Warszawa 2011, pp. 274-275.
[22] Yang R., He Y., Gao B., Tian G.,Y., Peng J.: Lateral heat conduction based eddy currenty thermography for detection of parallel cracks and rail tread oblique cracks. Measurement 66 (2015) pp. 54-61.

Received: 21.09.2015 *Paper reviewed* *Accepted: 05.01.2016*

Wojciech SAWCZUK, PhD, eng.

From 2010, an adjunct at the Institute of Combustion Engines and Transport of Poznan University of Technology, Faculty of Working Machines and Transportation. In his work deals with the scientific discipline which is the construction and operation of machines, specialty diagnostic machines. In particular research interests concern the research vibration braking of vehicles which run on rails, engine diagnostics and thermal tests of means of transport.

e-mail: wojciech.sawczuk@put.poznan.pl

Bartosz PAGÓREK

Od 2012 roku student Politechniki Poznańskiej na kierunku Transport Szynowy, Wydziału Maszyn Roboczych i Transportu. Główne zainteresowania to: budowa maszyn oraz związana z nimi eksploatacja, projektowanie części maszyn w programach typu CAD a także budowa pojazdów szynowych oraz infrastruktura kolejowa.

e-mail: bartoszpagorek@gmail.com